



ELSEVIER

Available online at www.sciencedirect.com

ScienceDirect

journal homepage: www.elsevier.com/locate/he

Hollow PdCu nanocubes supported by N-doped graphene: A surface science and electrochemical study

Zhengyu Bai ^{a,b}, Lu Niu ^a, Qing Zhang ^a, Hongjuan Feng ^a, Lin Yang ^{a,*}, Zongxian Yang ^b, Zhongwei Chen ^{a,c,**}

^a School of Chemistry and Chemical Engineering, Key Laboratory of Green Chemical Media and Reactions, Ministry of Education, Collaborative Innovation Center of Henan Province for Fine Chemicals Green Manufacturing, Henan Normal University, Xinxiang 453007, China

^b College of Physics and Electronic Engineering, Henan Normal University, Xinxiang 453007, China

^c Department of Chemical Engineering, University of Waterloo, Canada

ARTICLE INFO

Article history:

Received 1 February 2015

Received in revised form

6 August 2015

Accepted 12 August 2015

Keywords:

Alcohols oxidation

Hollow PdCu alloy nanocubes

N-doped graphenes

N species

ABSTRACT

N doped graphenes (NGs) are believed to be promising materials for constructing novel hybrid composites with desirable functionalities and applications in many fields. Therefore, a better understanding of the NGs holds the key to a better performance of the hybrid properties. A facile and low-cost preparation of NGs supported hollow PdCu alloy nanocubes (H–PdCu) catalysts were introduced in this paper. To increase the stability and efficiency of the catalysts, a two-step strategy was employed, which included the preparation of NGs and the synthesis of hollow PdCu alloy nanocube catalysts. A series of NGs using melamine, polypyrrole (ppy) and polyaniline (PANI) as nitrogen source, respectively. The influence of the different N species (pyridinic N, pyrrolic N and graphite N) on the morphologies and corresponding electrical properties of H–PdCu nanoparticles were studied. The results indicate that NGs are successfully synthesized, and hollow PdCu alloy nanocubes are well-dispersed on the surface of them with a relatively narrow particle size distribution. Electrochemical characterizations reveal that the H–PdCu/melamine-NG catalyst has excellent catalytic activity and stability toward alcohols oxidation in alkaline electrolyte, which can serve as promising anode catalysts in direct alcohols fuel cells (DAFCs).

Copyright © 2015, Hydrogen Energy Publications, LLC. Published by Elsevier Ltd. All rights reserved.

Introduction

Of the various types of fuel cells, the direct alcohols fuel cells (DAFCs), which are based on liquid fuels, have attracted

significant attention as a power source for portable electronic devices owing to its high energy density, low operating temperature and because it is non-toxic, which is not true for gaseous fuels [1–4]. However, lower oxidation activity of

* Corresponding author.

** Corresponding author. School of Chemistry and Chemical Engineering, Key Laboratory of Green Chemical Media and Reactions, Ministry of Education, Collaborative Innovation Center of Henan Province for Fine Chemicals Green Manufacturing, Henan Normal University, Xinxiang 453007, China. Tel.: +86 373 3326058; fax: +86 373 3328507.

E-mail addresses: yanglin1819@163.com (L. Yang), zhwchen@uwaterloo.ca (Z. Chen).

<http://dx.doi.org/10.1016/j.ijhydene.2015.08.029>

0360-3199/Copyright © 2015, Hydrogen Energy Publications, LLC. Published by Elsevier Ltd. All rights reserved.

alcohols and higher cost of Pt-based catalysts are the major drawbacks to limit DAFCs' practical application [5–7]. To solve these problems, tremendous efforts have been made to find catalysts with high activity, stability, and low cost.

On the one hand, less expensive and more abundant non-platinum catalysts with acceptable performance have been widely studied. For instance, Pd catalysts have been found to have good performance in alcohols oxidation, and therefore are considered as good candidates for DAFCs [8,9]. Multiple-component alloy with non-noble metals (Fe, Co, Ni, etc.) is one of the effective approaches to enhance the catalytic activity, and thereby reduce the loading of the noble metals and lower the cost of the Pd catalysts [10–12]. On the other hand, hollow metal nanospheres represent a new class of powerful catalysts because of their increased surface area, low density, easy recovery, self-supporting capacity, and surface permeability [13–15]. Till now, various hollow nanostructures such as hollow nanospheres [16–18], hollow nanotubes [19] have been prepared. Liu and his co-workers synthesized PtPd hollow nanospheres supported by Carbon nanotubes for formic acid electrooxidation [20]. Li et al. reported a carbon nanotube/raspberry hollow Pd nanosphere hybrids for methanol, ethanol, and formic acid electro-oxidation in alkaline media [21]. Obviously, design and synthesis of hollow alloy nanosphere catalysts represent a promising way to effectively improve the performance and utilization of catalysts, while the cost can be further decreased.

Meanwhile, the ideal support with large surface area, good conductivity and strong adsorption of metals shows the ability to improve the dispersion of metal nanoparticles, and thereby can enhance the utilization and efficiency of the noble metal electrocatalysts [22,23]. In this regard, graphenes are considered to be the ideal electrocatalyst support because they possess a large surface area, good thermal and chemical stability as well as great electrical conductivity [24,25]. However, the anchored metal nanoparticles tend to aggregate together due to the inefficient binding sites on the pristine graphenes surface for anchoring metal nanoparticles [26]. Therefore, N doped graphenes (NG) is generally prerequisite for further applications. Nitrogen doping onto the graphenes can effectively increase the active sites of the electrocatalysts [27,28]. With the introduction of the nitrogen, metal nanoparticles can be homogeneously anchored onto the support, leading to the generation of MeN_x (Me Co, Fe) active sites and thereby enhancing the electrocatalytic activity and utilization efficiency of the catalyst [29]. The studies show that the N species on the surface of graphenes can play an important role in controlling and regulating the shape and size of metal nanoparticles. However, there is scarce research about a systematic study on the influence of different N atom species in the formation course of hollow PdCu alloy nanocubes. Therefore, to further improve the performance of catalyst, it is very important to study the effect of the N atom species of the graphenes surface on the catalyst activity.

In this work, a series of NGs were synthesized by heat treatment process using polypyrrole (ppy), melamine and polyaniline (PANI) as the source of nitrogen, respectively. And hollow PdCu alloy nanocubes were prepared on the surface of the different N doped graphenes. The influence of the different N atom species (pyridinic N, pyrrolic N and

graphite N) on the morphologies and electrical properties of the catalysts were also studied. Electrochemical characterizations reveal that the H–PdCu/melamine-NG catalyst has excellent catalytic activity and stability toward alcohols oxidation in alkaline electrolyte, which can serve as promising anode catalysts in DAFCs.

Experimental

Preparation of different N doped graphenes

GO was prepared based on the modified Hummers' method [30]. The melamine-NG was synthesized via grinding and thermal annealing. GO and melamine were mixed together with a mass ratio of 1:1 under grinding for 2 h. The mixture was heated at 800 °C for 2 h under the protection of N₂. The final product was air-cooled to room temperature and labeled as melamine-NG.

The ppy-NG was synthesized by *in situ* chemical oxidative polymerization of pyrrole monomer and carbonization of the ppy. The GO (0.4 g) was dispersed in 50 mL ethanol aqueous solution (volume ratio 1:1) by ultrasonic treatment for 30 min. 80 mg pyrrole monomer was added to the above suspension and stirred for 10 min. Then 50 mL of Na₂S₂O₈ (2.289 g) aqueous solution was added slowly to the suspension with constant stirring for 12 h in ice-water bath. After reaction, the obtained ppy-GO powder was dried and heated at 800 °C for 2 h under the protection of N₂, which was labeled as ppy-NG.

The PANI-GO was prepared under the same condition except using aniline replaced pyrrole monomer. For comparison, the reduced graphene oxide (RGO) was also prepared under the same thermal treatment condition and labeled as PANI-NG.

Synthesis of hollow PdCu alloy nanocube catalysts

An aqueous solution of PdCl₂ (3.3 mg/mL, 3.8 mL), 20 mg of CuSO₄·5H₂O, and 50 mg of glutamate were mixed together in EG (50 mL) in 40 mL of EG. The pH of the system was adjusted to 11 by the dropwise addition of 8 wt% KOH/EG solution with vigorous stirring. Subsequently, 30 mg of the as-prepared melamine-NG were added, and the solution was ultrasonicated and stirred for 2 h to obtain a homogeneous suspension. Upon completion, the suspension was transferred into a 50 mL Teflon-lined stainless-steel autoclave. The autoclave was sealed, heated at 160 °C for 6 h, and air-cooled to room temperature. Finally, the product was collected by filtration and washed several times with DD water. The product was dried at 40 °C under vacuum for 8 h. The catalyst thus obtained was denoted as H–PdCu/melamine-NG. The H–PdCu/ppy-NG, H–PdCu/PANI-NG and H–PdCu/RGO were also prepared under identical conditions.

Characterization

The morphology of the samples was characterized by transmission electron microscopy (TEM) (JEOL-100CX) at 200 kV. The crystal structure of the products was analyzed by X-ray diffraction (XRD) recorded on a D/max-2200/PC X-ray

diffractometer with Cu K α radiation source. Field emission scanning electron microscope (FESEM) images and energy dispersive X-ray spectroscopy (EDX) results were obtained with ZEISS SUPRA 40 and X-MAX 20. The X-ray photoelectron spectroscopy (XPS) measurements were made using ESCA-LABMKLL electron spectroscope from VG Scientific (West Sussex, UK).

The electrochemical measurements in this study were conducted with a conventional three-electrode electrochemical cell on a CHI 660E electrochemical workstation. A glassy carbon electrode (3 mm o.d.) coating catalyst was used as working electrode, a saturated calomel electrode (SCE) was applied as the reference electrode and Pt foil (1 cm²) was used as the counter electrode. The cyclic voltammetric (CV) and chronoamperometry curves for ethanol or glycerol electrooxidation experiments were carried out in 1 M KOH containing 1 M ethanol or glycerol. Electrochemical CO-stripping voltammograms were conducted by bubbling CO into 0.5 M H₂SO₄ for 30 min at a potential of 0.1 V (vs. SCE electrode). All electrochemical experiments were performed at 25 ± 1 °C.

Electrochemical CO stripping voltammograms were obtained by oxidizing preadsorbed CO (CO_{ad}) in 0.5 M H₂SO₄ at a scan rate of 50 mV s⁻¹. CO was purged through 0.5 M H₂SO₄ for 30 min to allow complete adsorption of CO onto the catalyst. The working electrode was stayed at 0.1 V, and excess CO in

the electrolyte was removed by purging with high-purity N₂ for 30 min. The amount of CO_{ad} was evaluated by integrating the CO_{ad} stripping peak and correcting for the capacitance of the electric double-layer.

Results and discussion

The TEM images demonstrated that hollow PdCu nanocubes with a uniform size and distribution can be obtained with the different supports. Fig. 1 shows the TEM images of the as-prepared catalysts from H–PdCu/melamine-NG (a), H–PdCu/ppy-NG (b), H–PdCu/PANI-NG (c), and H–PdCu/RGO (d). As shown in Fig. 1a, the individual cubes are composed of an empty core with a uniform shell, and well-dispersed on the surface of support with a relatively narrow particle size distribution. The particle diameters vary from 40 to 65 nm, and the average diameter is about 50 nm. To better understand the formation mechanism of hollow nanocubes in our system, we have monitored their formation process by running the reactions under the same conditions but for different support. From Fig. 1(b–c), hollow PdCu nanocubes with a relatively narrow particle size distribution are evenly deposited on the surface of the supports, and no significant change in either the structure or composition can be observed. Fig. 1d shows the TEM image of the H–PdCu/RGO, in which little H–PdCu are

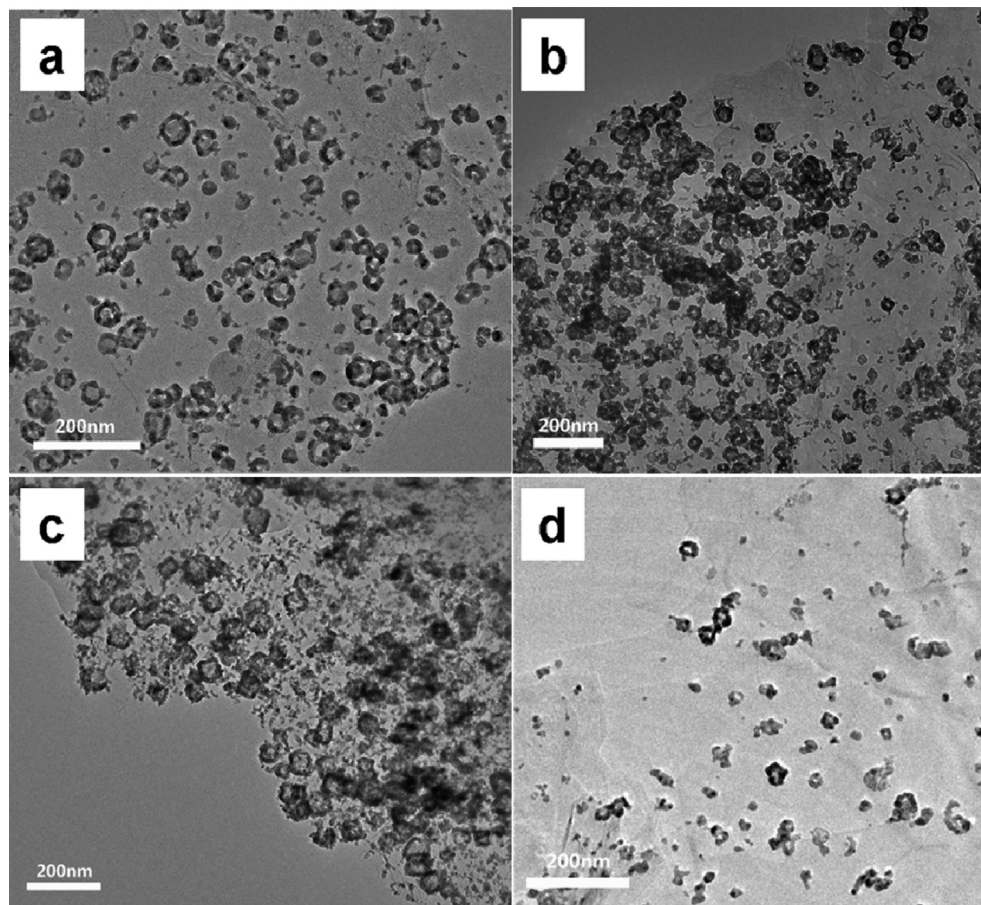


Fig. 1 – TEM images of the as-prepared catalysts from H–PdCu/melamine-NG (a), H–PdCu/ppy-NG (b), H–PdCu/PANI-NG (c), and H–PdCu/RGO (d).

formed, instead of abundant hollow nanocubes with a uniform shell and internal cavity. Additionally, compared with RGO, the morphology of NG is not changed obviously after doping by N and the presence of N appears to reduce the particles agglomeration. From the above results, it is believed that the graphenes doped by N is important for the formation of uniform H–PdCu catalysts with a good distribution.

The surface chemical states and elemental compositions of NG supports were analyzed by XPS. Fig. 2(a–c) shows the survey-scan spectra of melamine-NG, ppy-NG and PANI-NG, respectively. The survey-scan spectra of NG supports are mainly dominated by the signals of C 1s, N 1s and O 1s elements. The presence of N1s peak at about 400 eV demonstrates the successful incorporation of nitrogen in NG

supports, which is in good accordance with the results of EDX elemental mapping. The high resolution N 1s spectra of melamine-NG, ppy-NG and PANI-NG are shown in Fig. 2(d–f), respectively. All of the N1s spectra can be further deconvoluted into three peaks, which correspond to three individual N-containing species. The peak at about 400.1 eV can be assigned to pyrrolic N species from the pentagonal ring of ppy, 398.1 eV to pyridinic N, and 401.1 eV to graphitic N, respectively [31]. Pyridinic N and pyrrolic N represent nitrogen atoms bonding with two carbon atoms and donate one or two p-electron to the aromatic π -system. Graphitic N, also called “quaternary nitrogen”, refers to nitrogen atoms that substitute the carbon atoms in graphene layers [32]. Table 1 lists N species compositions of different NG supports determined

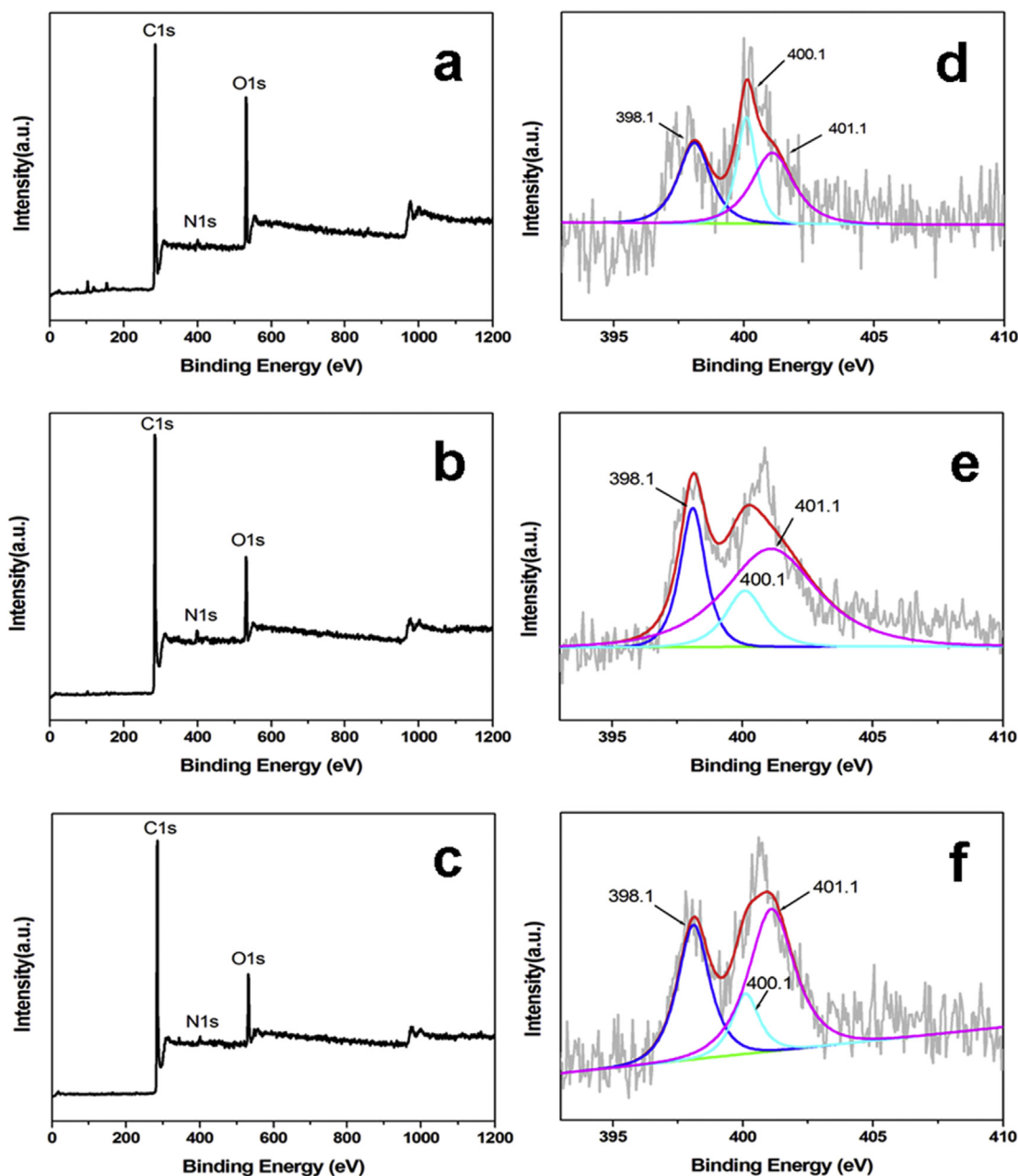


Fig. 2 – XPS spectra and the corresponding high-resolution N1s spectrum of the melamine-NG (a,d), ppy-NG (b,e), PANI-NG (c,f).

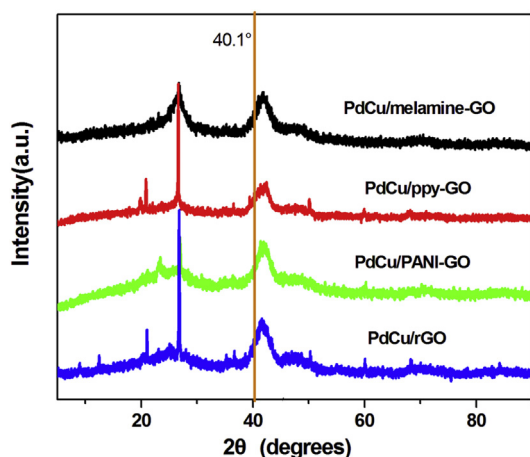
Table 1 – Nitrogen distributions of different samples.

Sample	N 1s (atom %)		
	pyrrolic N	pyridinic N	graphite N
melamine-NG	0.54	0.32	1.34
ppy-NG	0.55	0.43	0.63
PANI-NG	0.68	0.25	1.02

by XPS. It can be seen that melamine-NG, and PANI-NG include more pyridinic N, and graphitic N. As Table 1 shows, melamine-NG, ppy-NG and PANI-NG, both pyridinic N and graphitic N have been proposed to serve as active sites for nanomaterials (NMs) nucleation and retard NMs diffusion and aggregation [33]. More graphitic N and pyridinic N species on NG surfaces should be helpful to load the H–PdCu and enhance the catalytic activity of the H–PdCu/NG. This result is in good agreement with the value of electrochemically active surface area (EAS) of the catalysts.

Fig. 3 shows the XRD patterns of the as-prepared catalysts from H–PdCu/melamine-NG, H–PdCu/ppy-NG, H–PdCu/PANI-NG, and H–PdCu/RGO, respectively. As displayed in Fig. 3, Four peaks at 39.8°, 46.1°, 68.6° and 81.9° are characteristics of face-centered-cubic (fcc) crystalline Pd, which are corresponding to the facets (111), (200), (220), and (311), respectively. Obviously, different support has no significant influence on the crystalline form, and the peak positions of the H–PdCu/RGO slightly shift to higher angles in comparison with the Pd/RGO, which is ascribed to the formation of PdCu alloy. Additionally, the peak at 21.5° is detected in each case, which is attributed to the (002) planes of RGO, unlike the GO with a sharp peak centered at 10.2°, revealing the decreased interlayer distance from 0.71 to 0.34 nm [34]. This is due to the removal of oxygen-containing functional groups from the RGO. These observations demonstrate that the GO was efficiently transformed to RGO. Moreover, the XRD pattern of H–PdCu/NG is consistent with that of H–PdCu/RGO. It can be concluded that the crystal structure of RGO is not changed after N doping.

In order to investigate the distribution and content of the H–PdCu/NG composite, elemental mapping measurement were performed. Fig. 4 shows the SEM images and the

**Fig. 3 – XRD patterns of the as-prepared different catalysts.**

corresponding elemental mapping of the as-prepared catalysts from H–PdCu/melamine-NG (a), H–PdCu/ppy-NG (b), and H–PdCu/PANI-NG (c). On the mapping images of all samples, a homogeneous distribution of N, Pd and Cu elements can be clearly observed, except from C element. It can be seen that Pd and Cu of all samples are uniformly distributed in the mappings, which is in agreement with the TEM results. The N is well distributed on the mappings of melamine-NG, ppy-NG and PANI-NG, respectively. The results reveal that the graphemes were doped by N successfully and the N atoms are all homogeneous distributed in a series NGs. In the process of N dope, the N sources react with the oxygen functional groups like carbonyl, carboxyl, and lactone in GO to achieve the insertion of nitrogen and give more effective deoxygenation of GO. Therefore, the graphenes doped using melamine, ppy and PANI as N sources have a similar composition distribution and nanostructure.

The catalytic activity of the prepared catalysts towards alcohols oxidation under alkaline conditions was evaluated through electrochemical measurements. Fig. 5 shows the CV curves of H–PdCu/melamine-NG, H–PdCu/ppy-NG, H–PdCu/PANI-NG, and H–PdCu/RGO modified electrodes in 1 M NaOH solution containing 1 M ethanol (Fig. 5a), 1 M NaOH solution containing 1 M glycerol (Fig. 5b), respectively. The data were collected at a scan rate of 50 mV s⁻¹ from -0.8 to 0.2 V at 25 °C. And all the results were normalized on the basis of the amount of Pd loading (mass activity). As Fig. 5a shows, the ethanol electrooxidation is characterized by two well-defined current peaks on the forward and reverse scans. In the forward scan, the oxidation peak corresponds to the oxidation of freshly chemisorbed species which come from the ethanol adsorption. The reverse scan peak is primarily associated with the removal of carbonaceous species which are not completely oxidized in the forward scan. The value of the peak current in the forward scan represents the electrocatalytic activities of the electrocatalysts. Clearly, the maximum peak current density of the H–PdCu/melamine-NG catalyst (ca. 710 mA mg⁻¹) is much higher than that of the others. Fig. 5b is a comparison of corresponding CV curves for glycerol electrooxidation from the as-prepared different catalysts. From the curves, two main peaks for the glycerol electrooxidation are observed in both the forward and reverse scan directions. The mass values of H–PdCu/melamine-NG, H–PdCu/ppy-NG, H–PdCu/PANI-NG, and H–PdCu/RGO are 1300 mA mg⁻¹, 320 mA mg⁻¹, 450 mA mg⁻¹, and 186 mA mg⁻¹, respectively. It demonstrate that H–PdCu/melamine-NG modified electrode reveals extraordinarily high electrocatalytic activity relative to the electrode modified by other electrocatalysts, and the activities towards the ethanol and glycerol electrooxidation both decrease in the following order: H–PdCu/melamine-NG > H–PdCu/PANI-NG > H–PdCu/ppy-NG > H–PdCu/RGO. Both graphitic N and pyridinic N have been proposed to serve as sites for Pt nucleation and to retard Pt diffusion and particle coalescence. The abundance of graphitic N and pyridinic N species on NGs should assist the catalytic activity of catalysts. The total ratio of graphitic N and pyridinic N in melamine-NG, PANI-NG and ppy-NG is 1.66%, 1.27%, 1.06%, respectively. Therefore, H–PdCu/melamine-NG shows extraordinarily high electrocatalytic activity for alcohols oxidation.

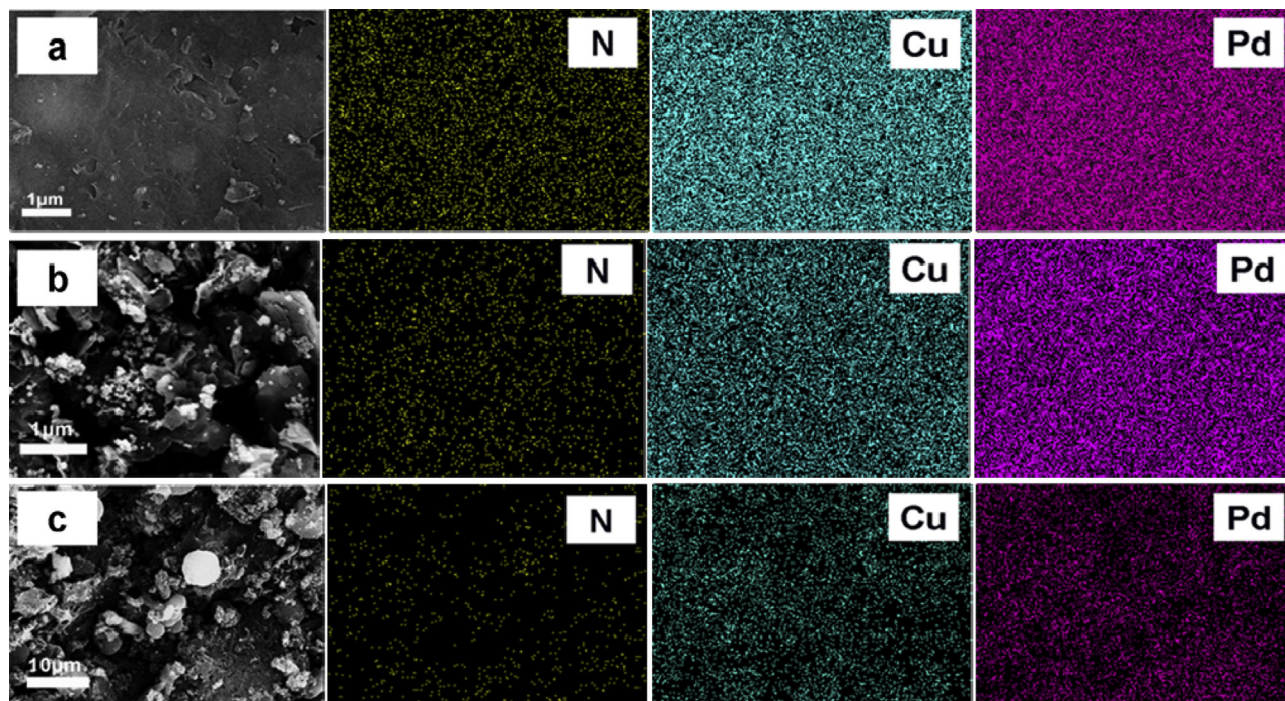


Fig. 4 – FESEM images and corresponding chemical mapping of the as-prepared catalysts from H-PdCu/melamine-NG (a), H-PdCu/ppy-NG (b), and H-PdCu/PANI-NG (c).

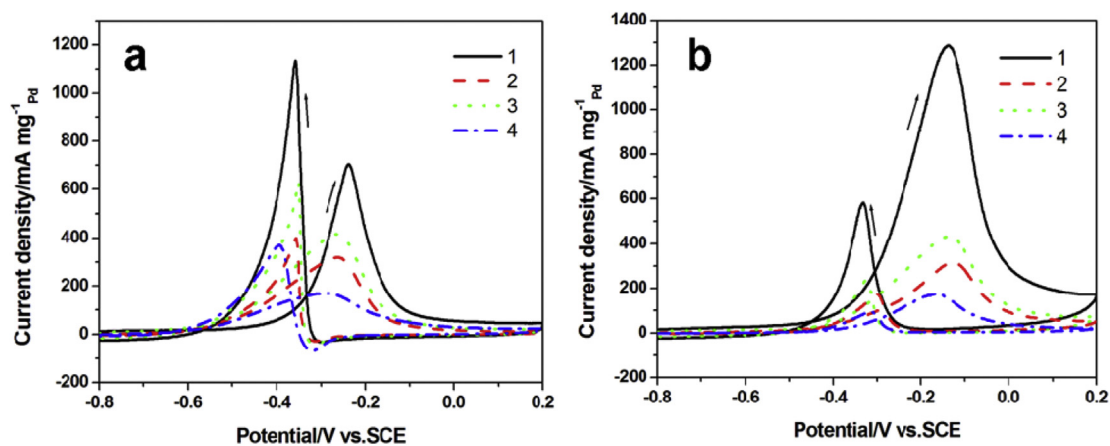


Fig. 5 – CV curves of the as-prepared catalysts from H-PdCu/melamine-NG (curve 1), H-PdCu/ppy-NG (curve 2), H-PdCu/PANI-NG (curve 3), and H-PdCu/RGO (curve 4) in different electrolytes: 1 M KOH + 1 M ethanol (a) and 1 M KOH + 1 M glycerol (b) aqueous solution, sweep rate of 50 mV s^{-1} , at 25°C .

In order to compare the electrochemical stability of the as-prepared catalysts for alcohols oxidation, chronoamperometry tests were carried out at -0.3 V for 6500 s in 1 M NaOH solution containing 1 M ethanol (Fig. 6a), 1 M NaOH solution containing 1 M glycerol (Fig. 6b), respectively. Evidently, the H-PdCu/melamine-NG catalyst shows much higher anodic currents and much slower degradation in currents, demonstrating better activity and stability than that of the other catalysts under the same conditions. The result further demonstrates that

the NG using melamine as N sources can significantly enhance the activity and stability of catalyst toward alcohols electrooxidation.

The electrochemical active surface area (EAS) of the catalysts was determined by CO-stripping CV measurements, which were performed in 0.5 M H_2SO_4 electrolyte at a scan rate of 50 mV s^{-1} . Fig. 7 shows the cyclic voltammograms obtained with CO adsorbed onto the catalysts (the solid curves) and without CO adsorbed onto the catalysts (the

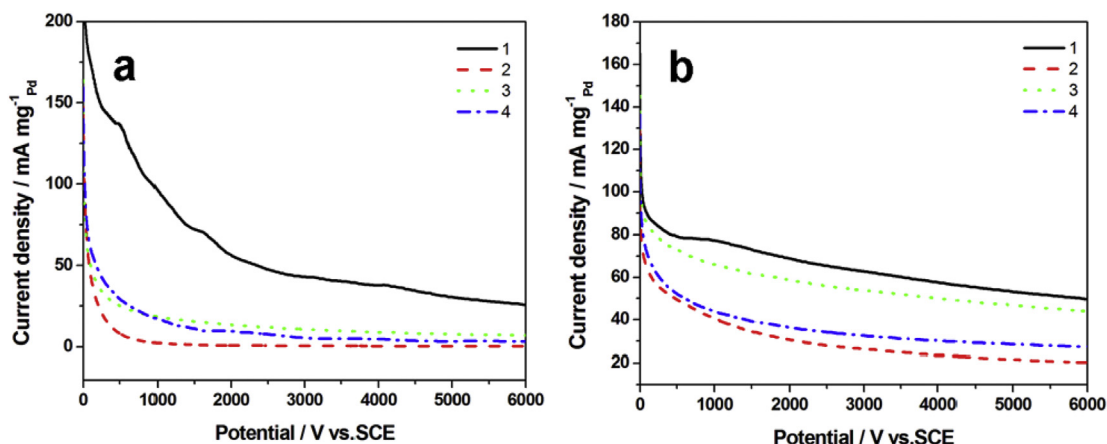


Fig. 6 – The chronoamperometry of the as-prepared catalysts from H–PdCu/melamine-NG (curve 1), H–PdCu/ppy-NG (curve 2), H–PdCu/PANI-NG (curve 3), and H–PdCu/RGO (curve 4) in 1 M KOH + 1 M ethanol (a), 1 M KOH + 1 M glycerol (b) aqueous solution, at a scan rate of 50 mV s^{-1} , at 25°C .

dashed curves) of H–PdCu/melamine-NG (a), H–PdCu/ppy-NG (b), H–PdCu/PANI-NG (c), and H–PdCu/RGO (d). The corresponding EAS of the catalyst was obtained from the following equation:

$$EAS = \frac{Q}{m \cdot C}$$

in which Q is the charge of the CO desorption–electrooxidation in microcoulombs (mC), m represents

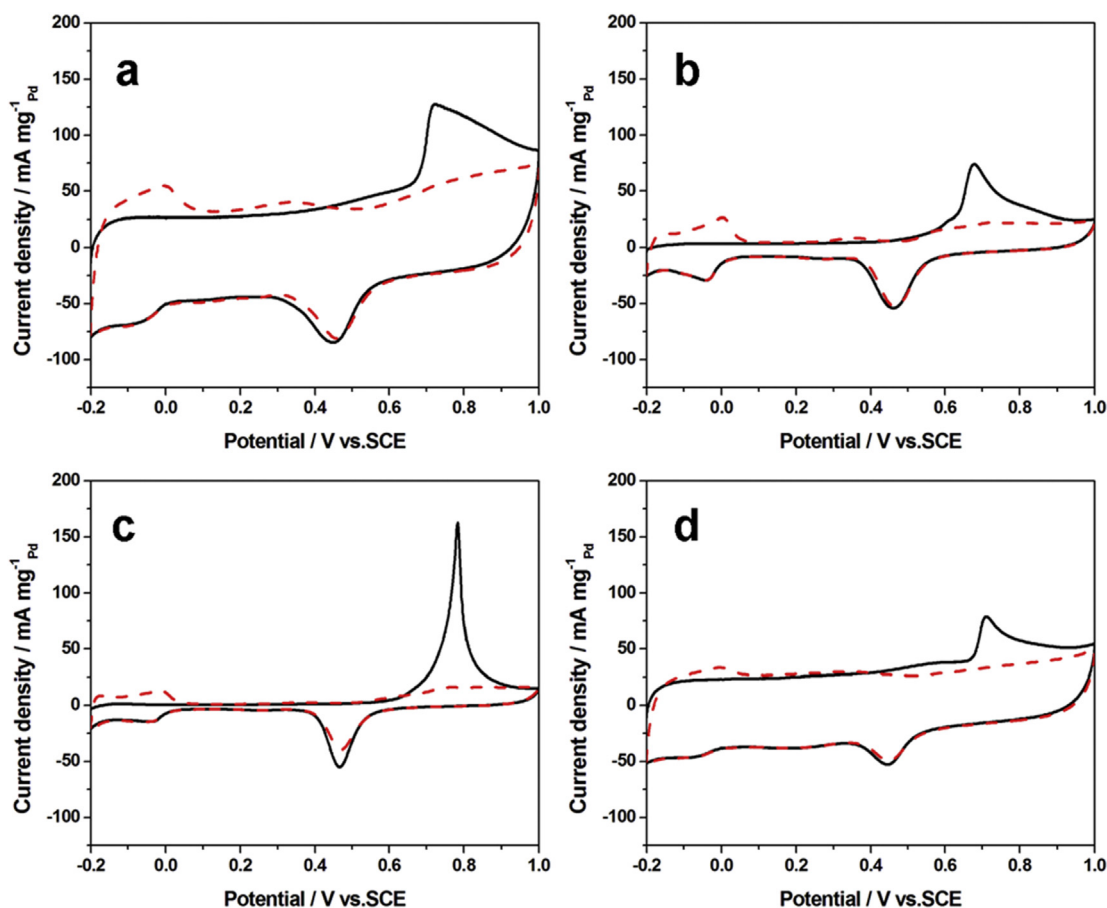


Fig. 7 – CV curves for the oxidation of preadsorbed CO at the as-prepared catalysts from H–PdCu/melamine-NG (a), H–PdCu/ppy-NG (b), H–PdCu/PANI-NG (c), and H–PdCu/RGO (d) in $0.5 \text{ M H}_2\text{SO}_4$, scan rate of 50 mV s^{-1} , at 25°C . Dashed curves were CVs for these electrodes without COad and solid curves for adsorbed COad.

the total amount of Pd (mg) on the electrode and C denotes the quantity of electricity when hydrogen molecules are adsorbed on Pd with a homogeneous and single layer (here, it is $420 \mu\text{C cm}^{-2}$). The calculated EAS was 426.81, 268.37, 330.46 and $137.64 \text{ m}^2 \text{ g}^{-1}_{\text{Pd}}$ for H–PdCu/melamine-NG, H–PdCu/ppy-NG, H–PdCu/PANI-NG, and H–PdCu/RGO, respectively. In addition, the activity varied in keeping with the same law as for alcohols oxidation. Obviously, it can further demonstrates that N doped graphenes can effectively increase the active sites, and thereby can enhance the catalytic activity and stability of the electrocatalysts.

Conclusions

In this work, a series of hollow PdCu alloy nanocubes supported on nitrogen-doped graphene support (H–PdCu/ppy-NG) were successfully synthesized using a simple one-pot template-free method. Compared with RGO, the NGs used as supports can provide more active sites and increase the dispersibility of H–PdCu, which could improve the electrocatalytic activity and utilization ratio of the catalyst. Additionally, different N source doped different mass ratio of N species in NGs. More pyridinic N and graphitic N species on NG surfaces should be helpful to load more H–PdCu for enhancing the catalytic activity of the H–PdCu/NG. H–PdCu/melamine-NG shows the highest catalytic activity and stability, which makes it the candidate for direct alcohols fuel cells catalysts.

Acknowledgment

This work was financially supported by the National Natural Science Foundation of China (21301051), Project funded by China Postdoctoral Science Foundation (2014061), and Young and Key Teacher of Henan Normal University.

REFERENCES

- [1] Xu C, Liu A, Qiu H, Liu Y. Nanoporous PdCu alloy with enhanced electrocatalytic performance. *Electrochem Commun* 2011;13:766.
- [2] Yi CG, Xu CW, Shen PK, Jiang SP. Effect of nitrogen-containing functionalization on the electrocatalytic activity of PtRu nanoparticles supported on carbon nanotubes for direct methanol fuel cells. *Appl Catal B Environ* 2014;140:158.
- [3] Zhao X, Yin M, Ma L, Liang L, Liu CP, Liao JH, et al. Recent advances in catalysts for direct methanol fuel cells. *Energy Environ Sci* 2011;4:2736.
- [4] Hsin YL, Hwang KC, Yeh CT. Poly (vinylpyrrolidone)-Modified graphite carbon nanofibers as promising supports for PtRu catalysts in direct methanol fuel cells. *J Am Chem Soc* 2007;129:9999.
- [5] Hogarth MP, Ralph TR. Catalysis for low temperature fuel cells part III: challenges for the direct methanol fuel cell. *Platin Met Rev* 2002;46:146.
- [6] Chen YG, Wang JJ, Meng XB, Zhong Y, Li RY, Sun XL, et al. Atomic layer deposition assisted Pt-SnO₂ hybrid catalysts on nitrogen-doped CNTs with enhanced electrocatalytic activities for low temperature fuel cells. *Int J Hydrogen Energy* 2011;36:11085.
- [7] Chen XT, Jiang YY, Sun JZ, Jin CH, Zhang ZH. Highly active nanoporous Pt-based alloy as anode and cathode catalyst for direct methanol fuel cells. *J Power Sources* 2014;267:212.
- [8] Bian CN. P.K.Shen, Palladium-based electrocatalysts for alcohol oxidation in half cells and in direct alcohol fuel cells. *Chem Rev* 2009;109:4183.
- [9] Dong Q, Zhao Y, Han X, Wang Y, Liu MC, Li Y. Pd/Cu bimetallic nanoparticles supported on graphene nanosheets: facile synthesis and application as novel electrocatalyst for ethanol oxidation in alkaline media. *Int J Hydrogen Energy* 2014;39:14669.
- [10] Xu CW, Shen PK, Liu YL. Ethanol electrooxidation on Pt/C and Pd/C catalysts promoted with oxide. *J Power Sources* 2007;164:527.
- [11] Li LZ, Chen MX, Huang GB, Yang N, Zhang L, Wang H, et al. A green method to prepare Pd–Ag nanoparticles supported on reduced graphene oxide and their electrochemical catalysis of methanol and ethanol oxidation. *J Power Sources* 2014;263:13.
- [12] Yang ZS, Wu JJ. Pd/Co bimetallic nanoparticles: coelectrodeposition under protection of PVP and enhanced electrocatalytic activity for ethanol electrooxidation. *Fuel Cells* 2012;12:420.
- [13] Feng YY, Liu ZH, Xu Y, Wang P, Wang WH, Kong DS. Highly active PdAu alloy catalysts for ethanol electro-oxidation. *J Power Sources* 2013;232:99.
- [14] Qi Z, Geng HR, Wang XG, Zhao CC, Ji H, Zhang C, et al. Novel nanocrystalline PdNi alloy catalyst for methanol and ethanol electro-oxidation in alkaline media. *J Power Sources* 2011;196:5823.
- [15] Lang HF, Maldonado S, Stevenson KJ, Chandler BD. Synthesis and characterization of dendrimer templated supported bimetallic Pt–Au nanoparticles. *J Am Chem Soc* 2004;126:12949.
- [16] Zhang H, Hao Q, Geng HR, Xu CX. Nanoporous PdCu alloys as highly active and methanol-tolerant oxygen reduction electrocatalysts. *Int J Hydrogen Energy* 2013;38:10029.
- [17] Stamenkovic VR, Mun BS, Arenz MK, Mayrhofer JJ, Lucas CA, Wang G, et al. Trends in electrocatalysis on extended and nanoscale Pt-bimetallic alloy surfaces. *Nat Mater* 2007;6:241.
- [18] Li SS, Lv JJ, Hu YY, Zheng JN, Chen JR, Wang AJ, et al. Facile synthesis of porous Pt-Pd nanospheres supported on reduced graphene oxide nanosheets for enhanced methanol electrooxidation. *J Power Sources* 2014;247:213.
- [19] Lv JJ, Zheng JN, Wang YY, Wang AJ, Chen LL, Feng JJ. A simple one-pot strategy to platinum–palladium@palladium core–shell nanostructures with high electrocatalytic activity. *J Power Sources* 2014;265:231.
- [20] Liu B, Li HY, Die L, Zhang XH, Fan Z, Chen JH. Carbon nanotubes supported PtPd hollow nanospheres for formic acid electrooxidation. *J Power Sources* 2009;186:62.
- [21] Liu ZL, Zhao B, Guo CL, Sun YJ, Shi Y, Yang HB, et al. Carbon nanotube/raspberry hollow Pd nanosphere hybrids for methanol, ethanol, and formic acid electro-oxidation in alkaline media. *J Colloid Interface Sci* 2010;351:233.
- [22] Liang HP, Guo YG, Zhang HM, Hu JS, Wan LJ, Bai CL. Controllable AuPt bimetallic hollow nanostructures. *Chem Commun* 2004;13:1496.
- [23] Liu ZL, Zhao B, Guo CL, Sun YJ, Xu FG, Yang HB, et al. Novel hybrid electrocatalyst with enhanced performance in alkaline Media: hollow Au/Pd core/shell nanostructures with a raspberry surface. *J Phys Chem C* 2009;113:16766.
- [24] Tan C, Huang X, Zhang H. Synthesis and applications of graphene-based noble metal nanostructures. *Mater Today* 2013;16:29.

- [25] Zhang QL, Zheng JN, Xu TQ, Wang AJ, Wei J, Chen JR, et al. Simple one-pot preparation of Pd-on-Cu nanocrystals supported on reduced graphene oxide for enhanced ethanol electrooxidation. *Electrochimica Acta* 2014;132:551.
- [26] Chen XM, Wu GH, Chen JM, Chen X, Xie ZX, Wang XR. Synthesis of “clean” and well-dispersive Pd nanoparticles with excellent electrocatalytic property on graphene oxide. *J Am Chem Soc* 2011;133:3693.
- [27] Favaro M, Agnoli S, Perini L, Durante C, Gennaro A, Granozzi G. Palladium nanoparticles supported on nitrogen-doped HOPG: a surface science and electrochemical study. *Phys Chem Chem Phys* 2013;15:2923.
- [28] Zhang LS, Liang XQ, Song WG, Wu ZY. Identification of the nitrogen species on N-doped graphene layers and Pt/NG composite catalyst for direct methanol fuel cell. *Phys Chem Chem Phys* 2010;12:12055.
- [29] Cai DD, Wang SQ, Lian PC, Zhu XF, Li DD, Yang WS, et al. Superhigh capacity and rate capability of high-level nitrogen-doped graphene sheets as anode materials for lithium-ion batteries. *Electrochimica Acta* 2013;90:492.
- [30] Geng DS, Chen Y, Chen YG, Li YL, Li RY, Sun XL, et al. High oxygen-reduction activity and durability of nitrogen-doped graphene. *Energy Environ Sci* 2011;3:760.
- [31] Wu JJ, Zhang D, Wang Y, Hou BR. Electrocatalytic activity of nitrogen-doped graphene synthesized via a one-pot hydrothermal process towards oxygen reduction reaction. *J Power Sources* 2013;227:185.
- [32] Shao YY, Zhang S, Engelhard MH, Li GS, Shao GC, Wang Y, et al. Nitrogen-doped graphene and its electrochemical applications. *J Mater Chem* 2010;20:7491.
- [33] Choi B, Yoon HS, Park IS, Jang JS, Sung YE. Highly dispersed Pt nanoparticles on nitrogen-doped magnetic carbon nanoparticles and their enhanced activity for methanol oxidation. *Carbon* 2007;45:2496.
- [34] Li SS, Hu YY, Feng JJ, Lv ZY, Chen JR, Wang AJ. Rapid room-temperature synthesis of Pd nanodendrites on reduced graphene oxide for catalytic oxidation of ethylene glycol and glycerol. *Int J Hydrogen Energy* 2014;39:3730.